

П.О. Коробко¹, А.В. Кузьмов^{1,2}

¹Інститут проблем матеріалознавства ім. І.М. Францевича НАН України;

²Національний технічний університет України "Київський політехнічний інститут імені Ігоря Сікорського".

ЕФЕКТИВНІ ПРУЖНІ ВЛАСТИВОСТІ ПОРИСТИХ МАТЕРІАЛІВ ЗІ СТРУКТУРОЮ ІНВЕРСНОГО ОПАЛУ

Базуючись на теоретичних засадах механіки композитів шляхом скінченно-елементного моделювання було досліджено ефективну пружну поведінку пористого матеріалу з періодичною структурою інверсного опалу. Здійснювалось осереднення питомої пружної енергії на представницькому осередку інверсного опалу за різних схем деформування. За рахунок цього було знайдено ефективні модуль зсуву та об'ємний модуль для різних випадків структури інверсного опалу. Виявилось, що ефективні модулі пружності вкрай чутливі до пористості. Зокрема нанесення додаткового покриття, навіть товщиною меншою від 0.05 діаметру сферичних пор (вихідних частинок полімеру), викликає збільшення ефективного об'ємного модуля пружності в 4 рази, а зсувного аж в 6 разів.

Ключові слова: метаматеріали, інверсний опал, представницький осередок, модулі пружності, мікромеханіка.

P. Korobko, A. Kuzmov

EFFECTIVE ELASTIC PROPERTIES OF POROUS MATERIALS WITH INVERSE OPAL STRUCTURE

Based on the theoretical principles of composite materials mechanics, the effective elastic behavior of a porous material with a periodic inverse opal structure was investigated by finite element modeling. The specific elastic energy was averaged on a representative cell of the inverse opal under different deformation schemes. This allowed us to find the effective shear modulus and bulk modulus for different cases of the inverse opal structure. It turned out that the effective elastic moduli are extremely sensitive to porosity. In particular, the application of an additional coating, even with a thickness less than 0.05 of the diameter of the spherical pores (the original polymer particles), causes an increase in the effective bulk modulus of elasticity by a factor of 4, and the shear modulus by a factor of 6.

Key words: metamaterials, inverse opal, representative cell, elastic moduli, micromechanics.

1. Introduction.

In recent years, intensive research has been conducted on the phenomena associated with the negative refractive index of electromagnetic waves [1]. The reason for the intensification of these studies was the emergence of a new class of nanostructured composite materials that have an ordered periodic structure and are called metamaterials. The structure of these materials can be changed so that they have a wider range of electromagnetic characteristics, including a negative refractive index. One type of metamaterials is porous materials with an inverse opal structure, and such materials are also being investigated as promising structural materials with high specific strength and stiffness characteristics [2]. Inverse opal structures, characterized by their unique geometry and mechanical properties, have emerged as a focal point in recent research due to their versatile applications. One notable advancement is in the domain of wound management, where inverse opal hydrogel layers incorporated into Chinese herb hydrogel patches have demonstrated significant improvements in mechanical properties. This development is crucial for medical applications, offering a promising pathway for the creation of advanced wound care solutions [3].

The inverse opal structure is made in several stages [4]. The first stage is the self-assembly of polystyrene spheres into an opal structure on a substrate by slowly evaporating the colloidal solution of these spheres. The second stage is sintering of the spheres to form a bond between them. The third stage involves electrodeposition of nickel to fill the remaining space between the spheres. The fourth stage is the etching of polystyrene to obtain the actual inverse opal structure, after which an additional layer of the same or another material can be applied to the formed structure. The periodic cell of the inverse opal is shown in Fig. 1.

Although the structure of the pore space in an inverse opal is quite complex, it can be characterized by only two parameters, such as the isthmus between spherical pores and the thickness of the coating applied to the metal frame, according to the material production technology. In this work, the porosity and thickness of the additionally deposited nickel layer are used as a characteristic of the structure. Nickel [4] is considered as a solid phase material for such a porous composite, both for the main structure and for the additional layer.

The Goal of this work is to find the effective elastic properties of materials with an inverse opal structure by finite element modeling on a unit cell.

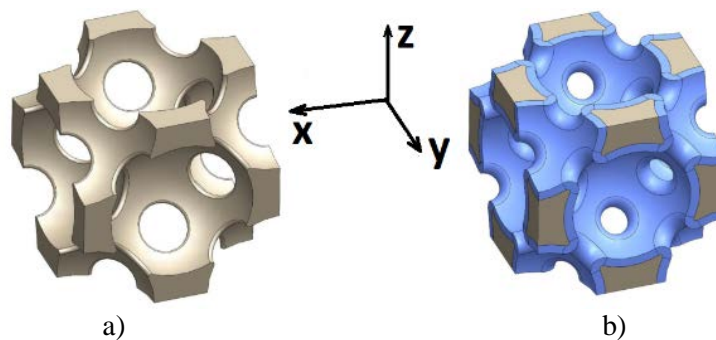


Fig. 1. Periodic cell of inverse opal a) uncoated; b) coated.

2. Micromechanical averaging procedure on a unit cell.

Inverse opal is a microheterogeneous material with a regular periodic structure. For composites of this type, approaches to finding effective properties are well developed [5]. For materials with a periodic structure, micromechanical averaging is sufficient to be carried out within a periodic cell, i.e., on a scale of heterogeneity that is smaller than the scale of the averaging length [6]. On the scale of the averaging length, the boundary of the representative cell is distorted close to a linear transformation [7], and in the case of an elementary periodic cell, generally speaking, it is not [8].

However, due to symmetry, in the case when there are no shear components of macroscopic "effective" deformations in the XYZ coordinate system shown in Fig. 1, the cell will retain a rectangular shape during such deformation. Using this, in the following, as a first approximation, we will consider the inverse opal as an isotropic composite. In this case, we assume that the main axes of the macroscopic stress and strain tensors are directed along the XYZ coordinate axes from Fig. 1. Accordingly, to describe the elastic behavior of the inverse opal, it will be sufficient to find only two independent elastic moduli, for example, the shear G and bulk K elastic moduli.

For this purpose, the elementary (representative) volume extracted from the material space is subjected to two loading schemes - hydrostatic compression and pure shear (Fig. 2.2).

To set up a numerical experiment to determine the effective elastic properties of a nanostructured material, it is necessary to use the properties of the solid phase of a porous material. In our study, the solid phase of the base and coating is electrodeposited nickel, the elastic constants of which correspond to the properties of pure nickel (Table 2.1).

Table 2.1

Solid phase material elastic properties

Material	Density, ρ	Young's Modulus, E	Poisson's ratio, ν
Electrodeposited nickel	8900 $\frac{kg}{m^3}$	171 GPa	0,31

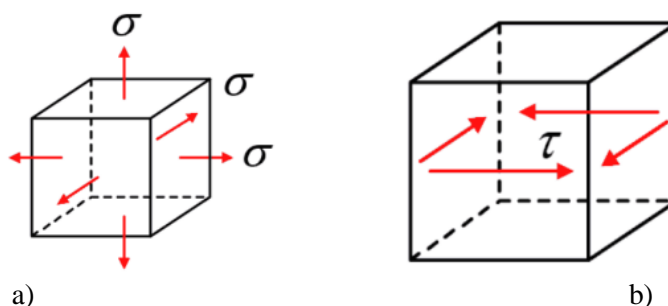


Fig. 2.2. Scheme of elementary volume loading: a) hydrostatic compression scheme; b) shear loading scheme.

As mentioned above, the structure must be subjected to hydrostatic and shear loading. In order to represent this mathematically, we have used the boundary conditions on the unit cell (UC), which are transformed into a strain matrix (e_{ij}^0) from which we can calculate the normal strain (e^0) and shear strain (γ^0) using the following formulas:

$$e^0 = e_{11}^0 + e_{22}^0 + e_{33}^0; \tag{2.1}$$

$$\gamma^0 = \frac{1}{\sqrt{3}} \sqrt{(e_{11} - e_{22})^2 + (e_{22} - e_{33})^2 + (e_{33} - e_{11})^2 + 6(e_{12}^2 + e_{23}^2 + e_{31}^2)} \tag{2.2}$$

Since the boundary of the elementary volume is a parallelepiped, considering the symmetry of the structure, the conditions for micromechanical averaging of a composite with a periodic structure can be represented in the form of displacements of the edges perpendicular to the axes of a rectangular coordinate system (Table 2.2). [5]

Table 2.2

Representative cell boundary conditions

Stress scheme	Boundary conditions	e_{ij}^0	e^0	γ^0
Hydrostatic	$\vec{n} = (1,0,0): U_1 = -X$ $\vec{n} = (0,1,0): U_2 = -Y$ $\vec{n} = (0,0,1): U_3 = -Z$	$e_{ij}^0 = \begin{vmatrix} 1 & 0 & 0 \\ 0 & 1 & 0 \\ 0 & 0 & 1 \end{vmatrix}$	3	0
Shear	$\vec{n} = (1,0,0): U_1 = X$ $\vec{n} = (0,1,0): U_2 = -Y$	$e_{ij}^0 = \begin{vmatrix} 1 & 0 & 0 \\ 0 & -1 & 0 \\ 0 & 0 & 0 \end{vmatrix} \equiv \begin{vmatrix} 0 & 1 \\ 1 & 0 \end{vmatrix}$	0	$\sqrt{2}$

3. Description of finite element modeling

The loading process is modeled by the finite element method in the ABAQUS/Standard software environment. The material model is assumed to be isotropic elastic, with the properties shown in Table 2.1. We apply displacements corresponding to the shear and hydrostatic loads to the elementary cell on the corresponding faces in accordance with the parameters given in Table 2.2. We use the automatic division of the solid phase of the structure into a mesh of ten-node quadratic tetrahedral finite elements by the type of volumetric stress. The results of modeling the hydrostatic compression of a structure with a pore diameter of 495 nm and a 33 nm nickel layer are shown in Fig. 2.3.

The target parameter for hydrostatic load modeling is the value of the total internal energy ALLIE accumulated during deformation. Having determined this parameter, we calculate the value of the total elastic specific energy from the following expression:

$$W = \frac{ALLIE}{V_c}, \quad (2.3)$$

where V_c – the volume of the representative cell.

On the other hand, the total elastic specific energy W is defined as [6]:

$$W = \frac{K}{2}(e^0)^2 + G(\gamma^0)^2, \quad (2.4)$$

where K – Bulk modulus, Pa; G – Shear modulus, Pa.

Taking into account the boundary conditions (Table 2.2), we can calculate the Bulk modulus K from formula (2.4) using the following formula:

$$K = \frac{2}{9} * W_h \quad (2.5)$$

where W_h – specific elastic energy accumulated as a result of hydrostatic compression, Pa.

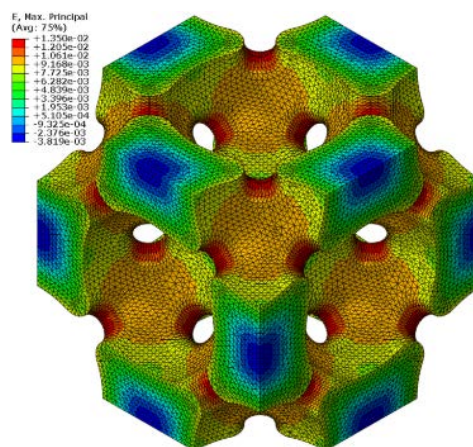


Fig. 2.3. Maximal strain under hydrostatic stress condition

Similarly to hydrostatic compression, we model the shear deformation (Fig. 2.4). The desired parameter in the shear load modeling is the value of the total internal energy ALLIE accumulated during

the deformation process. After determining this parameter, we calculate the value of the total elastic specific energy using formula (2.3).

Given the boundary conditions (Table 2.2), we can calculate the shear modulus G from formula (2.4) using the following formula:

$$G = \frac{1}{2} W_{sh} \tag{2.6}$$

where W_{sh} – specific elastic energy accumulated as a result of shear strain, Pa.

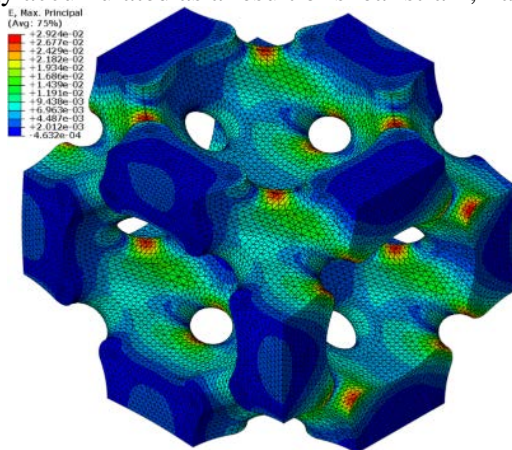


Fig. 2.4 Maximal strain under shear stress condition

The obtained values of the bulk modulus K and the shear modulus G fully describe the isotropic elastic behavior of the inverse opal structure under load. In Hooke's law for an isotropic linear elastic material, there is an unambiguous relationship between the elastic constants of the material, so the following dependencies are valid for determining the effective Young's modulus E^{eff} and Poisson's ratio ν^{eff} [9]:

$$E^{eff} = \frac{9KG}{3K + G}; \tag{2.7}$$

$$\nu^{eff} = \frac{3K - 2G}{2(3K + G)}. \tag{2.8}$$

Summarizing the values obtained from the finite element modeling with the results of analytical calculations in the form of a table (Table 2.3), while comparing them with the properties of the solid phase material.

Table 2.3

Numerical calculations results

Structure	Θ , %	W_h , [GPa]	W_{sh} , [GPa]	K , [GPa]	G , [GPa]	E , [GPa]	ν
Bulk Ni	0	-	-	-	-	171	0,31
NiIO 260nm	90	8,67	0,588	1,93	0,294	0,84	0,427
NiIO 520nm	84	21,5	2,53	4,77	1,27	3,49	0,378
NiIO 930nm	90	8,01	0,513	1,78	0,257	0,735	0,431
NiIO 470+19nm	65	79,3	14,4	17,6	7,2	19	0,32
NiIO 495+33nm	57	113	22,5	25,1	11,25	29,3	0,305

Conclusion: As can be seen from the calculation results, both the bulk and shear moduli of elasticity depend significantly on the structure of the inverse opal. The porosity of 0.9 is almost the limit for inverse opal and corresponds to a structure with thin cross-links. In this case, the stiffness of the inverse opal is about two orders of magnitude less than the stiffness of the solid phase material (i.e. nickel). In this case, the bulk modulus decreases less than the shear modulus. However, a slight decrease in porosity from 0,9 to 0,84 causes an approximately fivefold increase in the shear modulus and Young's modulus. The application of an additional layer causes an even more significant increase in the stiffness of the inverse opal. An additional coating, even with a thickness less than 0,05 of the diameter of the spherical pores (the original polymer particles), causes a 4-fold increase in the effective bulk modulus of elasticity and a 6-fold increase in the shear modulus.

References

1. Агранович В. М., Гартштейн Ю. М. Пространственная дисперсия и отрицательное преломление света // УФН. – 2006. – С. 1051–1068.

2. Rosario J. J., Berger J. B., Lilleodden E. T., McMeeking R. M., Schneider G. A. The stiffness and strength of metamaterials based on the inverse opal architecture // *Extreme Mechanics Letters*. – 2016. – Т. 12. – С. 86–96.
3. Cao X., Wang Y., Wu X., Wang J., Ren H., Zhao Y. Multifunctional structural color Chinese herb hydrogel patches for wound management // *Chemical Engineering Journal*. – 2024. – Vol. 485. – P. 149957. – ISSN 1385-8947. – DOI: <https://doi.org/10.1016/j.cej.2024.149957>.
4. Pikul J. H., Özerinç S., Liu B., Zhang R., Braun P. V., Deshpande V. S., King W. P. High strength metallic wood from nanostructured nickel inverse opal materials // *Scientific Reports*. – 2019.
5. Bakhvalov N.S., Panassenko G.P. *Upscaling: Averaging Processes in Periodic Media*. – Kluwer Academic Publishers, 1989.
6. Christensen R. M. *Mechanics of composite materials*. – New York: Wiley-Interscience, 1979. – 348 с.
7. Победря Б. *Механика композиционных материалов*. – Москва: Изд-во Моск. ун-та, 1984.
8. Kuzmov A., Olevsky E., Maximenko A. Multi-scale modelling of viscous sintering // *Modelling and Simulation in Materials Science and Engineering*. – 2008. – 16(3), 035002.
9. Божидарник В. В., Сулим Г. Т. *Елементи теорії пружності*. – Львів: Світ, 1994. – 560 с.